Paper

2-dimensional analysis of settlement damage to masonry buildings caused by tunnelling

G. Liu,
BSc, DPhil
Ove Arup & Partners

Professor G. T. Houlsby,
FREng, MA, PhD, CEng, FICE
Department of Engineering Science, University of Oxford

C. E. Augarde,
MSc, DPhil, CEng, MICE
School of Engineering, University of Durham (Formerly Department of Engineering Science, University of Oxford)

Keywords:
masonry, tunnelling, settlement, modelling, facades, cracking

Synopsis

In current practice, estimating the effects of tunnel construction in soft ground beneath an existing building is usually a two-stage procedure, where interaction between the ground and the building is ignored. This paper describes a study of tunnelling-induced settlement damage to masonry buildings, using a numerical model, in which interaction is included. 2-dimensional finite elements(FEs) are used with non-linear material models for the soil and for a masonry facade. The excavation of a tunnel is simulated, and the resulting damage in the facade, principally cracking, can be observed. This study concentrates on the effect of facade weight and stiffness and the horizontal location of the facade with respect to the tunnel axis. The study finds that increasing facade weight tends to increase damage, owing to the larger horizontal strains. Increasing facade stiffness, however, appears to reduce damage, since the differential settlements under the facade are inhibited.

Introduction

Tunnelling is frequently used to build transportation links and other infrastructure in urban areas. However, the excavation of a tunnel induces ground deformations that may affect existing structures.

Although the resulting ground settlements rarely cause major structural damage to buildings, aesthetic and serviceability damage may occur[1]. Structures adjacent to a new tunnel, in particular old masonry buildings, may suffer damage resulting in costly repairs or require expensive protective measures, such as underpinning or compensation grouting.

These consequences of tunnelling activities have prompted recent research into improved methods for predicting the ground movements induced by tunnelling and assessing the influence of tunnelling on adjacent structures, particularly for sensitive masonry buildings.

The current practice for settlement damage assessment is basically a two-stage approach. First, the ground movements induced by tunnelling are estimated assuming 'greenfield' conditions, with no buildings present. Estimates are made using semi-empirical methods[2,3], FE analysis[1] or physical experiments. The resulting greenfield settlement trough is then applied to the building and the resulting damage assessed. The building is typically modelled as a simple beam[2,4].

However, this approach is based on the greenfield settlement profile, without any consideration of the interaction between the building and the ground. The presence of a building will modify the settlement beneath and will also, in many cases, reduce horizontal movement[5].

Therefore, other approaches, which attempt to include the interaction between the building and ground, have been developed to predict settlement damage. The simplest coupled model is a simple beam or a frame on 'Winkler ground' (ground modelled as elastic springs), which is subject to a greenfield settlement profile. A more sophisticated model is described by Simpson[5], where a masonry facade, consisting of solid masonry, windows and attached floorslabs, is modelled by a combination of several 'strata' with different stress–strain relationships. To simulate the interaction between the facade and the ground, a cushion of ground is placed between a 'remote' greenfield settlement profile and the structure itself.

Although these models are able to provide some useful insights into the ground–structure interaction, they still assume that the effects of the building are confined to a zone near the ground surface.

Potts & Addenbrooke[4,6] have modelled an existing building as a weightless elastic beam on the ground surface. In this study, the ground is simulated with 2-dimensional FEs having a non-linear elasto-plastic material constitutive model. This is an attempt to investigate the interaction between the ground and a building. However, an elastic beam model does not account for any non-linearity of response of a real building (e.g. due to cracking in a masonry structure) and cannot therefore represent the behaviour of a real building during the construction of a tunnel. It also emerges in the research reported here that the weight of the building itself may be important.

The methods currently used in practice, to assess the damage to masonry buildings due to tunnelling, do not take account of the interaction between the building and the ground, which is clearly of some importance. Generally, these methods tend to overestimate the potential damage and therefore may lead to unnecessary, and costly, protective measures.

The passage of tunnel construction beneath a building creates a 'wave' of settlement; accurate prediction of damage therefore ideally requires a 3-dimensional numerical model. 3-dimensional models are currently under development by the authors[7] but they remain computationally expensive and probably beyond the reach of practising engineers.

This paper reports a study of tunnelling-induced settlement damage using 2-dimensional FEs which lies between current practice and research and 3-dimensional models. The modelling in this study accounts for interaction between a masonry building and the ground and uses a realistic constitutive model for masonry. The use of non-linear models for both the soil and masonry are the main advances over previous work. The study is restricted to simple masonry facades founded on uniform stiff clay through which an unlined tunnel is constructed, although the results provide interesting insights into the behaviour of facades generally when subjected to tunnelling settlements.

Components of the numerical model

Soil model and properties

Short-term settlements are generally recognised to be of prime importance in determining structural damage[2]; the soil behaviour is therefore modelled as undrained (or incompressible). A nested yield surface model proposed by Houlsby[8] is used to model the features of London clay in this study. This model is elasto-plastic and takes into account the large changes in stiffness that occur at small strains for overconsolidated clays, now recognised to be important for accurate modelling[9]. The model also incorporates the effect of stress history on the current stiffness. Similar soil models, based on kinematic hardening, have been developed in recent years[9,10].

This soil model includes several yield surfaces in the shape of von Mises yield surfaces in stress space. Each surface can be translated in stress space by the stress point when it touches the surface. The outermost failure surface is a von Mises yield sur-

face which is fixed in the stress space. The sizes of the yield surfaces are governed by the stress–strain hardening law used in the model. The initial positions of the yield surfaces are set up on the basis of the past stress–strain history of the soil.

The properties are determined by the bulk elastic modulus, the shear modulus, and the undrained shear strength s_u, as usual for a von Mises model. For a nested yield surface model consisting of n surfaces, the inner n - 1 surfaces require n - 1 pairs of strength c_i and hardening parameters h_i (i = 1,2 ... n - 1). These are usually described by dimensionless parameters $c'_i = c_i/s_u$, $h'_i = h_i/G$. The hardening parameters h'_i can be replaced by the more straightforward parameters $g'_i = G_i/G$ which are the dimensionless tangential shear stiffnesses after a specific surface is activated. Fig 1 shows the variation in stiffness with strain amplitude given by the combination of parameters c'_i, g'_i for the

Surface	c_i'	h_i'	g_i'
1	0.02	9	0.9
2	0.04	4.5	0.75
3	0.06	1.5	0.5
4	0.1	0.75	0.3
5	0.15	0.6	0.2
6	0.2	0.6	0.15
7	0.3	0.3	0.1
8	0.5	0.1	0.05
9	0.7	0.05	0.025

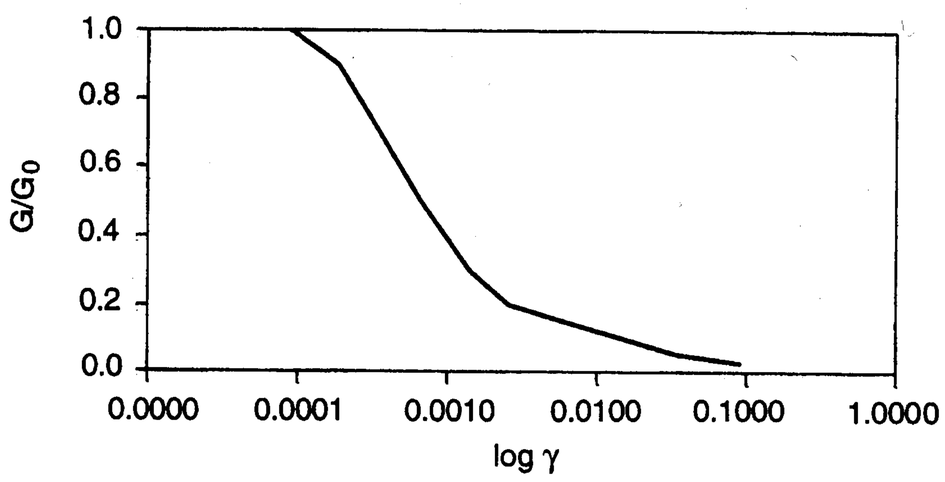

10-surface model used in this study. (In Fig 1, G_0 is the shear modulus at very small strain and γ is the shear strain.)

The parameters above define the shape of the stiffness–strain relationship for the soil. Magnitudes of shear moduli and undrained strength, for use in the FE model, are derived from data for London clay from a site at Victoria Embankment, London, investigated by St John *et al* [11]. The undrained shear strength s_u and shear modulus G are taken to increase linearly with depth, z, below the ground surface, by the following relations:

$$s_u = s_{u0} + \rho z = 60 + 6z \quad \text{....(1)}$$

$$G = G_0 + \lambda z = 30\,000 + 3000z \quad \text{....(2)}$$

where
ρ and λ are constants having dimensions kPa/m
s_{u0} and G_0 are the undrained strength and
small strain modulus at the surface $z = 0$

The ground water table is assumed to lie at the surface (z = 0). The site investigation[10] found that K_0, the coefficient of earth pressure at rest, varied from 1.0 to 1.5. Thus K_0 is assumed for simplicity to be 1.0 in this study. The unit weight of the saturated clay γ_s is taken as 20kN/m^3. Therefore, the initial horizontal and vertical stresses are linearly increasing with depth. These soil properties are used for all analyses presented in this paper.

Elastic no-tension model for masonry

The choice of constitutive model for masonry in the facades studied in this paper is of prime importance. Interaction between facade and ground is likely to be strongly affected by cracking, and hence change of stiffness, of the facade. Masonry can be characterised as non-homogeneous and anisotropic, having very high compressive strength and little tensile strength. Two main approaches have been adopted in the past for numerical modelling of masonry structures using FEs. The first models each brick and mortar joint separately[12]; this is, however, unsuitable for the majority of real structures. An alternative chosen by many researchers[13] is to treat the masonry as homogeneous and to use a constitutive model that reflects the behaviour of bricks and mortar combined. This is the approach taken here, and the behaviour is simplified to that of a material with infinite compressive strength and near zero tensile strength[14]. Other methods, such as those based on rigid block analysis[15], have the advantage that they provide improved modelling of the individual units of masonry and their relative rotations and translations. These models are not, however, based on conventional FE procedures and, at present, cannot be incorporated into a conventional FE analysis.

Fig 1. The nested surface model for stiff clay

An elastic no-tension macroscopic model is used in this study to simulate the behaviour of a masonry material. In addition, the cracks that can develop in the material are smeared across the cracked element or a part of it. It is assumed that the material behaves elastically when it is in compression and cracks when and where tension develops[14].

This non-linear behaviour is accommodated in the FE solution algorithm employed in this study as follows. At the end of each load step, the principal stresses are checked at each element integration point. If both the principal stresses are compressive, the material is intact and elastic properties are adopted. If the major principal stress is tensile, but the minor one is still compressive, a single crack is expected along the direction normal to the major principal direction and the material loses its stiffness along that direction, while it still behaves elastically in the other direction. Once both principal stresses are tensile, double cracking appears and the material loses its stiffness totally at that integration point.

To ensure numerical stability of the solution, the post-cracked stiffness of the masonry material is set to a small value (1% of the original stiffness) rather than zero. Also, the loss of stiffness after cracking is implemented gradually rather than suddenly.

In the elastic no-tension model, the total strain is decomposed into the elastic and cracking strains. The cracking strain is used to assess the degree of damage. It is assumed that visible cracking occurs when the cracking strain is greater than 500$\mu\varepsilon$.

FE models

The study presented here uses the same simple tunnel configuration and masonry facade throughout. The facade is located normal to the tunnel axis, but its horizontal location with respect to the tunnel is altered in some of the later analyses. The facade is 20m wide and 8m high. It has 10 openings, representing windows (each 1.5m × 2m high) and a doorway (2m × 3m high). The tunnel is 5m in diameter and is situated with its axis at a depth of 10m below the surface.

The foundation supporting the facade is not modelled in this study. The presence of a foundation would lead to a stiffer response of the building to the tunnelling settlements. However, most of the older masonry buildings likely to be of interest in tunnelling settlement damage predictions are supported on shallow strip foundations which can be expected to provide relatively little flexural resistance as compared with a modern reinforced concrete footing. Foundations of this nature were discovered in the investigations of the Mansion House, London, prior to tunnelling works[1].

The facade is modelled with plane stress FEs (six-noded triangles) with unit thickness. To prevent instability, linear elastic lintels 0.4m in depth, having a high tensile strength, are placed above the openings in the facade (see Fig 2). Both elastic lintels and uncracked masonry have the same modulus, E = 10^{7}kPa, and Poisson's ratio, ν = 0.2. The unit weight of both materials is γ_b = 20kN/m^3.

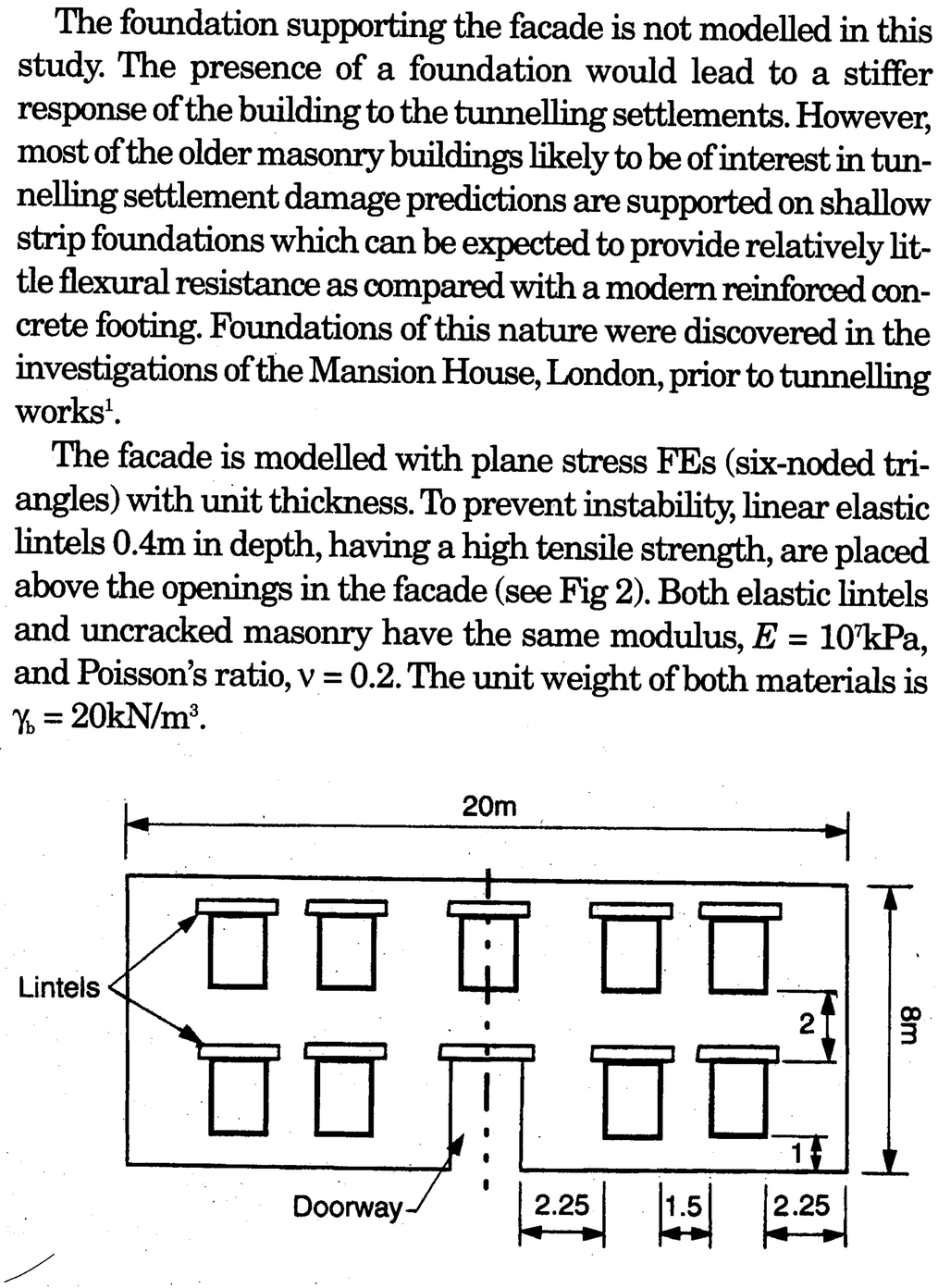

Fig 2. Facade layout

The ground is modelled by plane strain FEs (also six-noded triangles) with unit thickness. The nodes of the facade and the ground are numbered independently, and tie elements as described by Houlsby *et al*[16] are used to join the facade and ground meshes together. This is necessary, as the dimensionality of the meshes differs. The model therefore assumes no slip between the facade base and the ground.

The choice of an appropriate equivalent thickness of the zone of the ground analysed is one of the key issues in 2-dimensional analysis of this sort of problem. The 'correct' thickness can be assessed only by modelling the 3-dimensional aspects of the problem. This is one of the main reasons for carrying out the much more complex 3-dimensional analyses. Nevertheless, 2-dimensional analysis can be used for some simple parametric studies.

Symmetric layout

To save on computing time, symmetry is exploited in the analyses where the centre of the facade is located above the tunnel axis. In these cases, only half of the facade and half of the ground block are analysed. The meshes used for the ground in the symmetric case contain 201 elements and 446 nodes. The facade mesh contains 248 elements and 577 nodes. Since a 16-point numerical integration scheme is used to calculate the element stresses, there are a total of 3216 stress integration points in the facade, giving a fine resolution. Fig 3 shows the boundary conditions imposed on the meshes. Along the side boundary of the soil block, the nodes have zero horizontal displacement but are free in the vertical direction. At the base, all nodes are fully fixed. In addition, a symmetrical boundary condition is imposed on the nodes in the facade along its centreline.

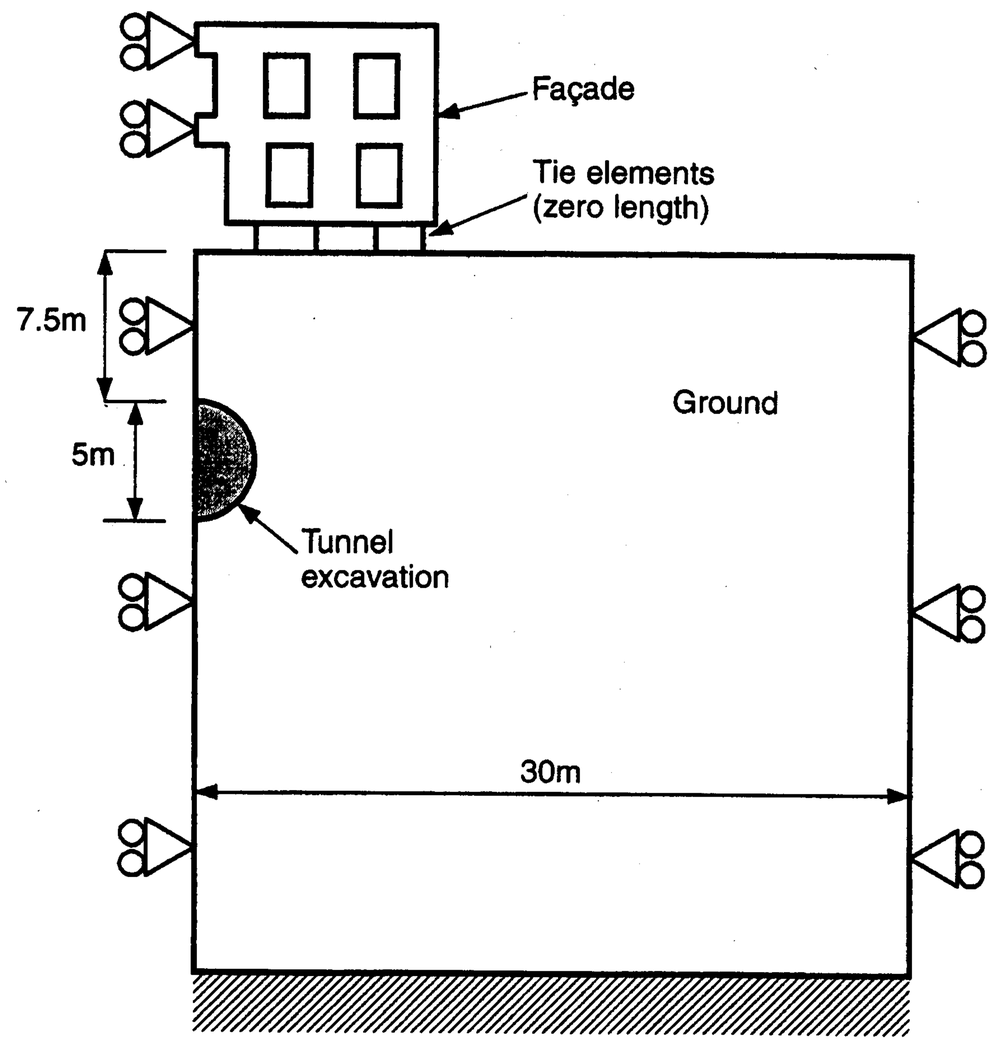

Fig 3. Boundary conditions for the ground and facade in symmetric cases

Unsymmetric layout

In the unsymmetric case, the whole facade and ground block must be analysed. The mesh for the facade is the same as in the symmetric case but includes the reflection. The mesh for the ground used in the unsymmetric case is similar to that for the symmetric analysis but represents a 140m × 50m block of soil. The same tie elements as used in the symmetric case are applied to join the soil mesh to the facade mesh. The boundary conditions for the ground are the same as before, but the symmetry requirement for the building is no longer needed. The position of the facade is controlled by its eccentricity x which is defined as the distance between the centreline of the facade and the tunnel axis (Fig 4).

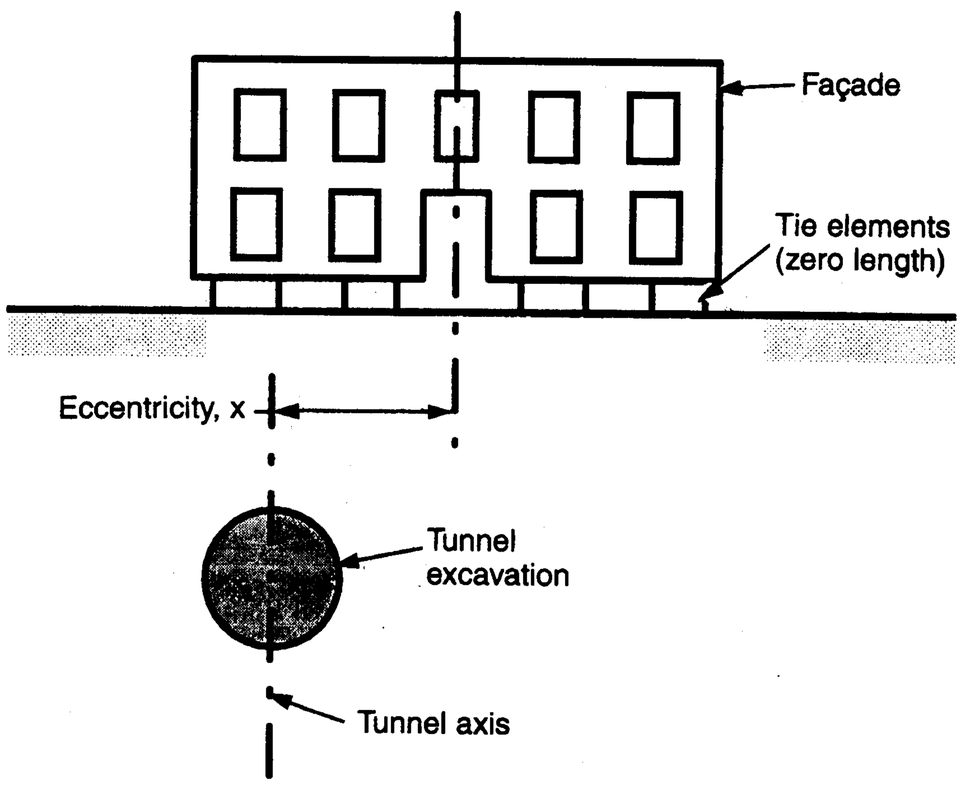

Fig 4. The layout of the model in unsymmetric cases

Simulation of tunnelling

Prior to excavation, the self-weight of the soil is balanced by initial stresses in the ground. The self-weight of the building is then applied and the state of the masonry material in the facade is monitored. Once the facade self-weight has been applied in full, the displacements in the ground and facade are reset to zero before excavation begins. The state variables (representing the stress history in the masonry and the soil) are, however, preserved. Therefore, displacements predicted with the model are due only to the excavation, and account is taken of the existing state of the building and ground prior to tunnelling. The excavation of an unlined tunnel is simulated by removing soil elements within the tunnel area and by applying loads to the excavated faces to remove surface tractions[17]. The entire process is assumed undrained. This means that the effects of consolidation of the soil beneath the building before tunnel construction have been ignored. Note also that the foundation of the building is not modelled, although clearly this would influence the results.

A comparison of uncoupled and coupled damage assessments

This section compares damage predictions from the numerical model for two analyses of the same symmetric layout of facade and tunnel. In the first, the 'uncoupled' case, a greenfield settlement trough is obtained from the model and is then imposed on the facade. (This approach is similar to the methods currently used in practice.) In the second 'coupled' case, the tunnel is excavated while the building is present on the surface.

An uncoupled analysis

The greenfield settlement trough obtained from the FE model, without a building, is shown in Fig 5. The trough is similar to the Gaussian profile predicted by standard empirical approaches[2,3], although wider, with the point of the inflection at approximately 7m from the axis.

Taking the settlements predicted for the region below the building from the profile of Fig 5 and applying them to the facade, with horizontal fixity at the base, gives the cracking patterns seen in Fig 6(a). The threshold level below which cracks are not plotted is a cracking strain of 500με, as outlined earlier. It should be noted that the number of crack lines plotted represents the magnitude of the cracking strain at that element integration point. This method of displaying crack data occasionally results in crack lines lying slightly outside the facade, as will be evident in later plots. Fig 6(b) shows the compressive stress trajectory (i.e. the directions of the minor principal stress) at the element integration points. The length of the lines indicates relative stress magnitude. It can be seen that the building arches across the settlement trough, with major amounts of cracking.

A coupled analysis

The cracking pattern and stress trajectory for the coupled case

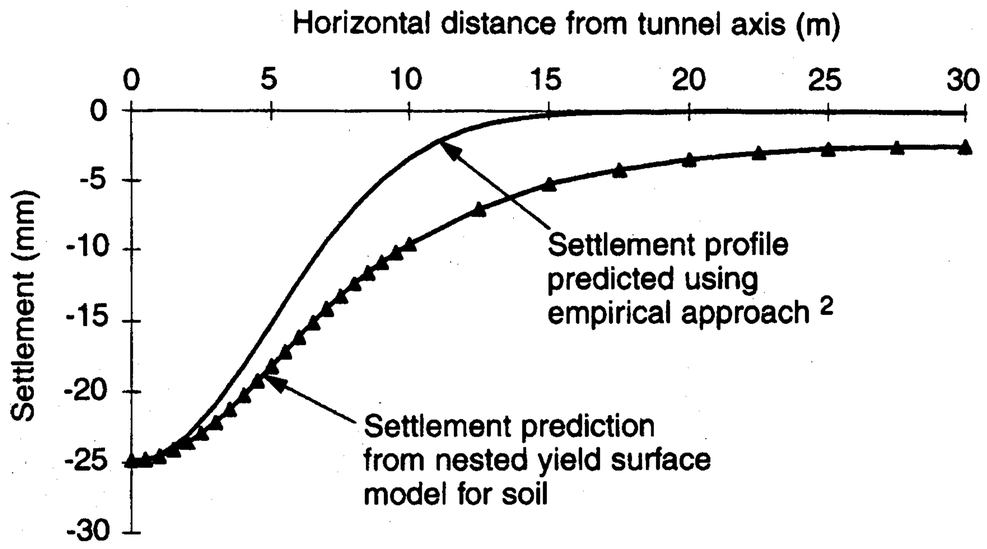

Fig 5. Greenfield settlement troughs

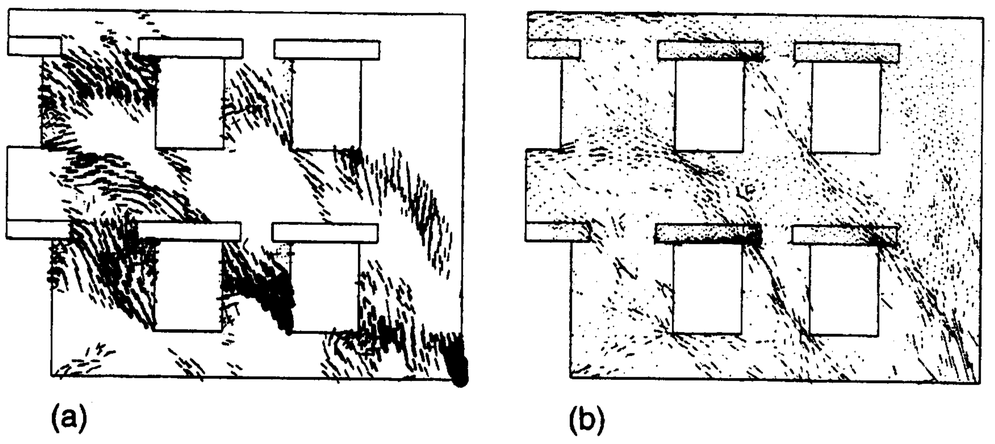

(a) (b)

Fig 6. Cracking pattern and stress trajectory for the uncoupled analysis

are shown in Fig 7(a) and (b). Again, the stress trajectory plots show that the differential settlements force an arching effect in the masonry material of the facade. Two 'stress arches' are visible in the uncoupled analysis, while three are visible in the coupled analysis.

Cracking damage

Significant differences are apparent between the cracking pattern predicted for the coupled and uncoupled analyses. First, the coupled analysis predicts less serious damage in the building, as expected. In addition, the cracking pattern is quite different to the uncoupled analysis. At the first-floor level, the cracking pattern is similar to the uncoupled case, with the cracks parallel to the stress arches. On the ground floor the dominant cracking pattern is vertical, implying the existence of large, tensile horizontal strains at the base.

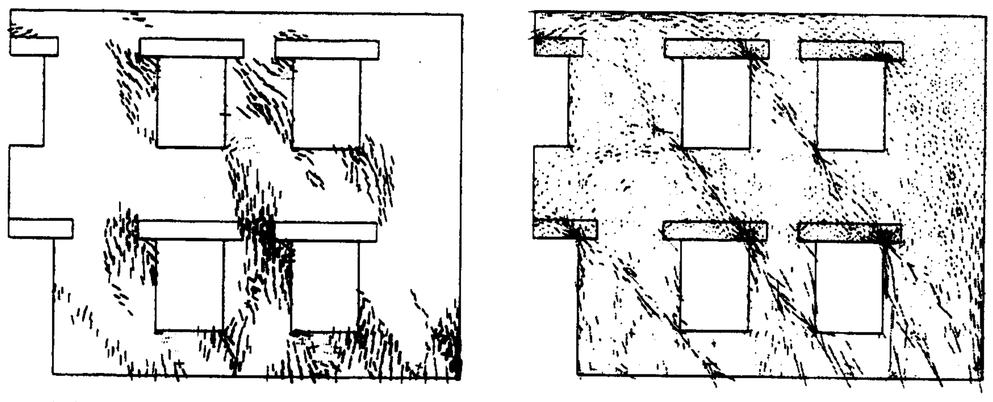

(a) (b)

Fig 7. Cracking pattern and stress trajectory for the coupled analysis

Ground movements and soil state changes

Fig 8 shows the horizontal and vertical ground movements for both analyses. The most obvious difference is the higher settlement beneath the building in the coupled analysis. Outside the building, heave is observed, resulting from the incompressible soil behaviour. The settlement trough underneath the facade in the coupled analysis is roughly divided into three small flat steps corresponding to the alignment of the windows. In contrast to the inward horizontal movement in the uncoupled analysis, the coupled analysis shows outward horizontal movement beneath the facade, probably because it moves into the ground and pushes the soil laterally. The horizontal movement profile is also divided into three parts, corresponding to the steps in the settlement. The positions of the separating points appear to coincide with the three stress arches visible in Fig 7(b). Inside each arch, the ground is stretched, leading to the vertical cracks in the facade.

The state of the soil during an analysis can be examined by plotting the number of activated yield surfaces. Fig 9 shows the state of the ground after excavation, for the uncoupled and coupled analyses. After excavation, more yield surfaces are activated around the tunnel in the coupled case, because application of the weight of the facade to the ground has led to the activation of some surfaces prior to excavation. Another important feature

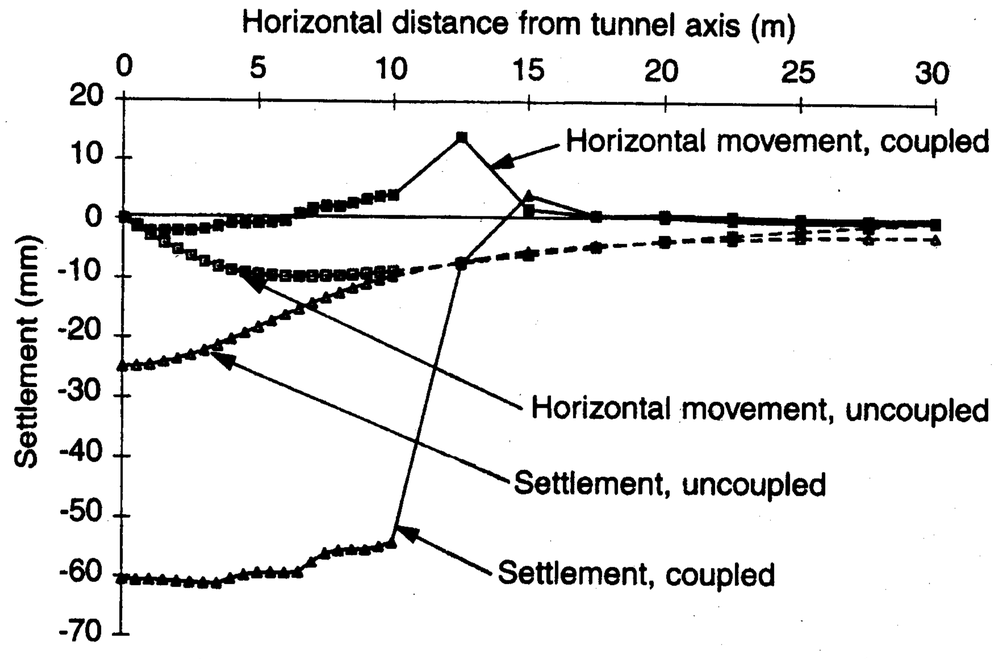

Fig 8. Ground movements in the uncoupled and coupled analyses

of the coupled plot is the presence of a highly plastic area, where nine surfaces are activated, located at the corner of the facade.

The larger settlements in the coupled analysis can also be explained in terms of the state of the ground prior to excavation. In the uncoupled analysis, shear stresses above the tunnel are low, resulting only from the self-weight of the soil. In the coupled case, shear stresses are much higher, owing to the additional presence of the facade. The stiffness of the soil in the coupled case is, therefore, much lower since more yield surfaces have been activated by the higher shearing before excavation. A stress concentration at the corner of the facade leads to the development of regions where all inner state surfaces in the soil model are activated, implying a potential failure surface.

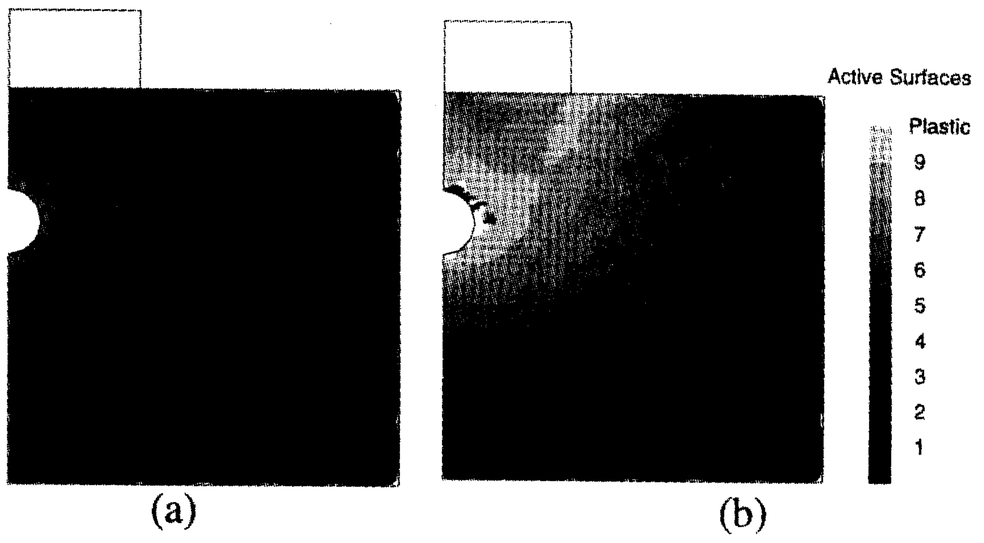

(a) (b)

Fig 9. States in ground after excavation for uncoupled and coupled analyses

As pointed out earlier, the depth of the 2-dimensional analysis is important. A 1m-thick facade on a 1m-thick block of the ground tends to overestimate the stresses in the ground. In addition, the long-term consolidation after the construction of the building would be expected to reduce the stresses in the ground at the ends of the building. The comparison of these analyses does, however, provide some indication of the ground movement trends. Possible interaction mechanisms between a building and the ground are also suggested by examining the state of the soil.

A parametric study

The study outlined serves to show the key role of the interaction between building and ground in an assessment of tunnelling settlement damage. This section of the paper will examine the effects on the predicted damage of varying the stiffness, weight and position of the building. Given the number of parameters defining the geometry and properties used in an analysis, it is possible to cover only a few simple cases. Various dimensionless groups are, however, used to widen the applicability of the results presented here. In particular, the tunnel depth is kept relatively shallow and constant throughout, since the settlement trough produced becomes wider and flatter as depth increases, thus reducing the differential settlements at the surface and the consequent interactions.

Symmetric cases

First, symmetric cases are considered. The settlement and horizontal movement, the stiffness of the facade, and the unit weights of the facade and ground, are normalised into the following groups, respectively, as

$$\delta' = \frac{\delta}{D}\frac{G_0}{\gamma_s D}, u' = \frac{u}{D}\frac{G_0}{\gamma_s D}, (Et)' = \frac{Et}{G_0 D},$$

$$(\gamma_b t)' = \frac{\gamma_b t}{s_{u0}}, (\gamma_s)' = \frac{\gamma_s Z}{s_{u0} + \rho Z} \quad \text{....(3)}$$

where

D is the tunnel diameter (5m)

Z is the depth to the tunnel axis

δ and u are the settlement and horizontal movement

(The other nomenclature is as given previously.)

Thus the dimensionless movements, δ', u',will be a function of

$$f((Et)', (\gamma_b t)', (\gamma_s)') \quad \text{....(4)}$$

The parameters for 17 test problems are summarised in Table 1, where the dimensionless settlements δ' are also given (at the facade centre and the maximum). The test number consists of

three digits. The second (1,2,3,4) and third (1,2,3,4) digits stand for the four different values of $(\gamma_b t)'$ and $(Et)'$, respectively. Test 200 is an uncoupled analysis, while other problems are coupled analyses. (According to this numbering method, the analyses described in the previous section of this paper are 200 and 233.) The significant aspects of the results are now described.

Arching effects

All coupled tests show three major stress arches in the facade roughly located at the same positions as the coupled analysis in the previous section. These arches play an important role in the interaction between the building and the ground. An explanation for the flatter troughs found with coupled analyses can be made in terms of these arches, as can the changes in behaviour as the weight and stiffness of the facade are changed.

The formation of arches results in the redistribution of the pressure on the ground from the building. Since the weight of the building has been carried already by the soil before excavation, the net extra load between building and the ground due to excavation is zero. Therefore, ground located under the arches will sustain a higher pressure than other areas. Consequently, soil under the arches will settle more than elsewhere, leading to a flatter settlement trough. In addition, the larger vertical force will cause a stress concentration near the arch supports in the ground that may cause the local failure of the soil close to the foundation.

In addition, the horizontal thrust of the arches will push the soil outwards and cause horizontal tensile strain and vertical cracking in the facade base.

TABLE 1: Summary of the test problems in the parametric study ($(\lambda_s)'=1.667$)

No.	$\lambda_b t$ (kN/m²)	$(\lambda_b t)'$	Et (kN/m)	$(Et)'$	δ'_{max}	δ'_{centre}
200	0	0	0	0	1.49	1.47
211	3	0.05	1.5×10^6	10.00	1.33	1.33
212	3	0.05	5.0×10^6	33.33	1.24	1.24
213	3	0.05	1.0×10^7	66.67	1.19	1.17
214	3	0.05	1.5×10^7	100.00	1.16	1.13
221	10	0.1667	1.5×10^6	10.00	1.94	1.89
222	10	0.1667	5.0×10^6	33.33	1.92	1.86
223	10	0.1667	1.0×10^7	66.67	1.84	1.81
224	10	0.1667	1.5×10^7	100.00	1.83	1.80
231	20	0.3333	1.5×10^6	10.00	3.84	3.77
232	20	0.3333	5.0×10^6	33.33	3.72	3.66
233	20	0.3333	1.0×10^7	66.67	3.67	3.63
234	20	0.3333	1.5×10^7	100.00	3.65	3.62
241	30	0.5	1.5×10^6	10.00	9.25	9.07
242	30	0.5	5.0×10^6	33.33	8.67	8.59
243	30	0.5	1.0×10^7	66.67	8.42	8.34
244	30	0.5	1.5×10^7	100.00	8.40	8.34

The effect of the building weight $(\gamma_b t)'$

The weight of the building has the most significant effect on the depth of the settlement trough under the facade. Fig 10 shows the settlement profiles for analyses with varying values, demonstrating this clearly. An increase in $(\gamma_b t)'$ results in greater loss of stiffness locally in the ground, owing to activation of yield surfaces, hence leading to larger settlements during excavation. This effect can be seen in Fig 11 where the ground state is plotted for analyses 213 and 243.

The arching in the facade also changes with $(\gamma_b t)'$. As Fig 12 shows, the arches produced are flatter when parameter $(\gamma_b t)'$ is low. As the building weight increases, the arches become higher. The low arches confine the cracked area mainly within the ground floor and leave the upper part of the facade intact, as indicated in the crack patterns for analyses 213 and 243 in Fig 13.

Fig 13 also shows much greater horizontal cracking in the base of the heavier facade. This can be explained as an effect of the higher arches and the loss of the lowest arch (see Fig 12) leading to increased horizontal thrust and consequent vertical cracking.

The effect of facade stiffness $(Et)'$

The value of $(Et)'$ is not found to alter the depth of the settlement

Fig 10. Settlement profiles obtained for selected analyses

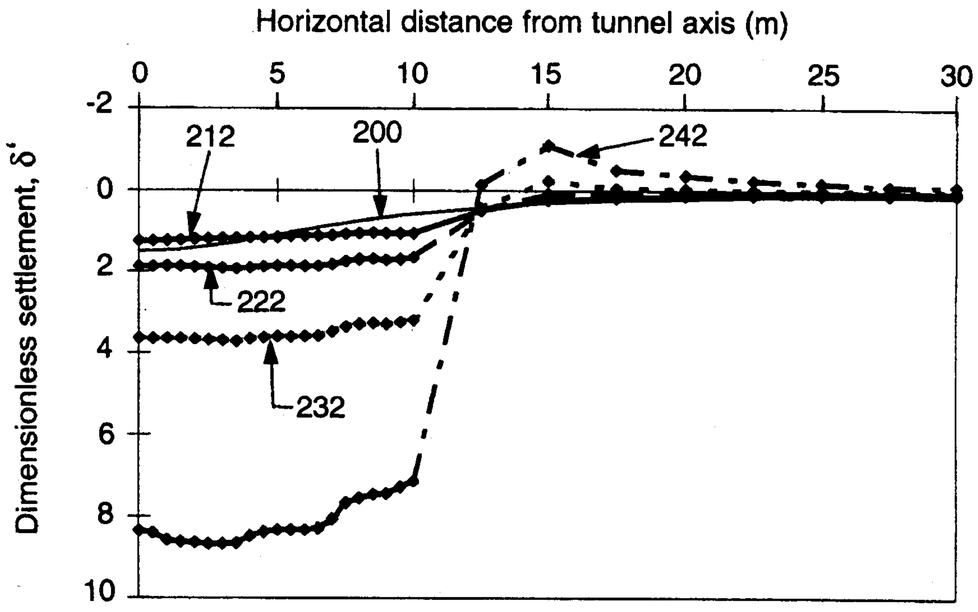

Fig 11. States in ground with differing $(\gamma_b t)'$: (a) 213, (b) 243

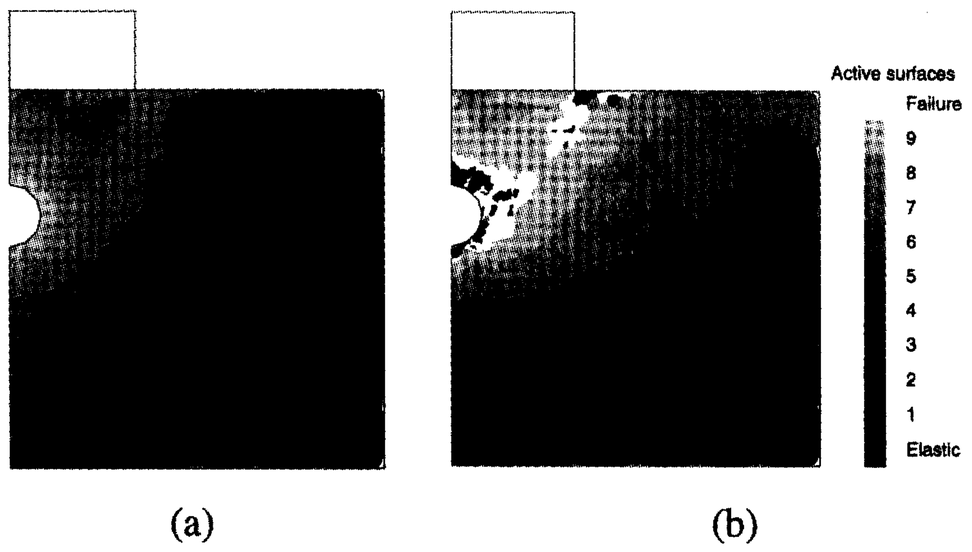

troughs, but does have a strong influence on the damage in the facade. Again, this can be explained by the formation of load-bearing arches in the facade.

The test problems show (although the results are not reproduced here for brevity) that smaller values of $(Et)'$ yield more uniform pressures between the facade and the ground, as might be expected. This means that the arches produced with lower stiffness facades will be more diffuse, with consequently less restraint to the ground settlement. Therefore, such a facade will experience more serious damage, from the greater differential settlements. This trend is clearly seen in crack patterns for analyses 211 and 214 (Fig 14) with $(Et)'$ varying from 10 to 100. The cracking damage in the area near A is due to the settlement and is noticeably reduced by increasing $(Et)'$.

Unsymmetric cases

The effect of the position of the facade is studied here with 11 analyses, as summarised in Table 2. Two values for the unit weight of the facade material and five values of the eccentricity x of the facade centreline with respect to the tunnel axis are considered. The results are presented using the same dimensionless parameters as used for the symmetric case, with the addition of a dimensionless eccentricity, $e = x/Z$.

Ground movements

Figs 15 and 16 show settlement profiles for analyses with the two facade unit weights. These plots show that, as eccentricity is increased from $e = 0$ to $e = 0.5$, the location of maximum settlement moves from the centre point of the facade to one end and

Fig 12. Stress trajectory plots in facades with differing $(\gamma_b t)'$: (a) 213, (b) 243

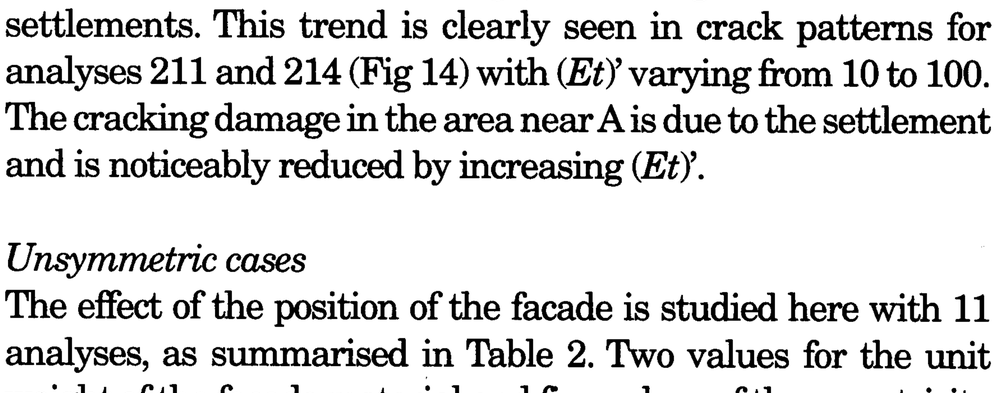

Fig 13. Cracking patterns for facades with differing $(\gamma_b t)'$: (a) 213, (b) 243

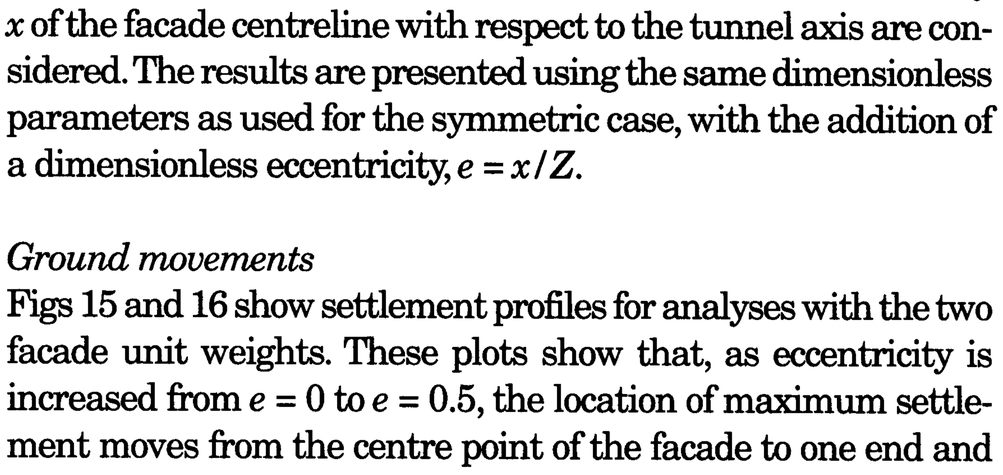

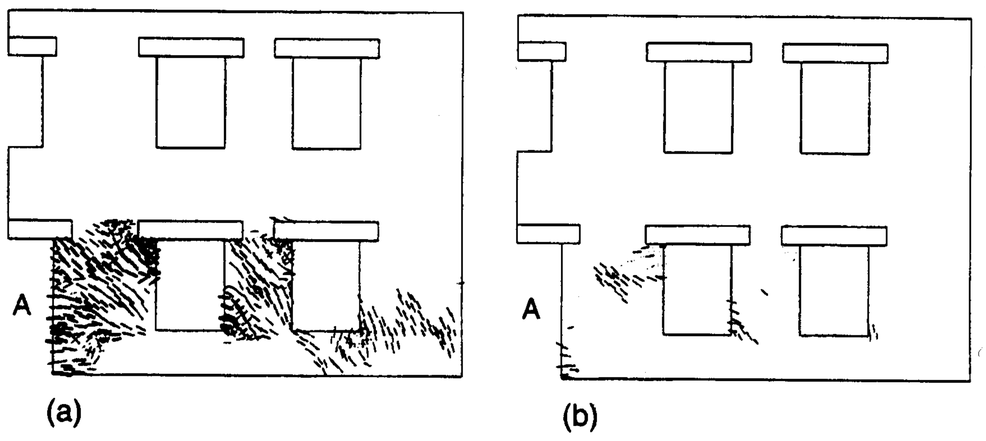

Fig 14. Cracking patterns for facades with differing (*Et*)': (a) 211, (b) 214

its magnitude increases dramatically. When $e = 0.5$, the dimensionless settlements reach maximums of 3.25 and 8.58 for the two unit weights. These settlements are 1.69 and 2.02 times the equivalent settlement values in the symmetric case. In addition, considerable tilts of 2.2:1000 and 6.5:1000 are also observed at these eccentricities.

Fig 17 shows the state of the soil beneath the facade for three values of the eccentricity. When $e = 0.5$, a highly activated band extends from the tunnel to the left edge of the facade. Since the state number along this band reaches 9, a potential failure plane develops. These observations may be explained with reference to the possible mechanism for upper-bound failure discussed by Davis *et al*[18] who suggest possible block failure mechanisms for a tunnel excavated under a greenfield site. It might be expected that, when one edge of the facade coincides approximately with one failure surface of a possible upper-bound failure mechanism of the ground alone, the effect of the building would be to increase greatly the tendency of the ground to fail along such a mechanism, leading to large settlement and tilt of the building. When $e = 2$, there is considerably less activation of yield surfaces in the ground, although areas approaching plasticity are evident at the facade edges.

When the facade lies entirely to one side of the centreline of the tunnel, the settlement under the facade is decreased considerably, becoming less than that in the symmetric case. Beyond

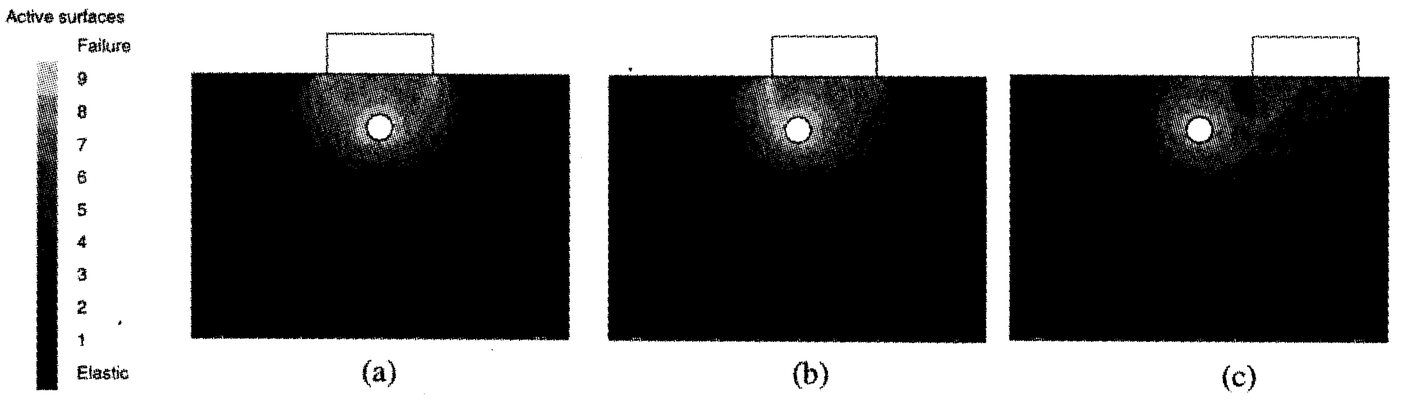

Fig 17. Soil states for analyses with a light facade and varying facade eccentricity (a) $e = 0$, (b) $e = 0.5$, (c) $e = 2.0$

TABLE 2: Summary of the test problems with differing horizontal positions of the facade

No.	$\lambda_b t$ (kN/m²)	$(\lambda_b t)'$	Et (kN/m²)	e	δ'_{max}	Position (m)
u200	0	0	na	na	1.41	0.0
u223a	10	0.1667	1.0×10^7	0	1.93	0.0
u223a1	10	0.1667	1.0×10^7	0.5	3.25	-5.0
u223b	10	0.1667	1.0×10^7	1	2.81	0.0
u223b1	10	0.1667	1.0×10^7	1.5	1.51	5.0
u223c	10	0.1667	1.0×10^7	2.0	1.16	1.0
u233a	20	0.3333	1.0×10^7	0	4.25	3.5,-3.5
u233a1	20	0.3333	1.0×10^7	0.5	8.58	-5.0
u233b	20	0.3333	1.0×10^7	1.0	5.80	0.0
u233b1	20	0.3333	1.0×10^7	1.5	2.55	5.0
u233c	20	0.3333	1.0×10^7	2.0	1.34	15.0

the point of inflection, the greenfield trough shows a hogging region (Fig 5). However, the trough under the facade always exhibits a sagging mode, even in this area, which is hogging in the greenfield case. This can be explained by the fact that the stress induced by the self-weight of the building controls the ground movements underneath the building in the area far from the tunnel centreline. This effect is local for light facades, as the

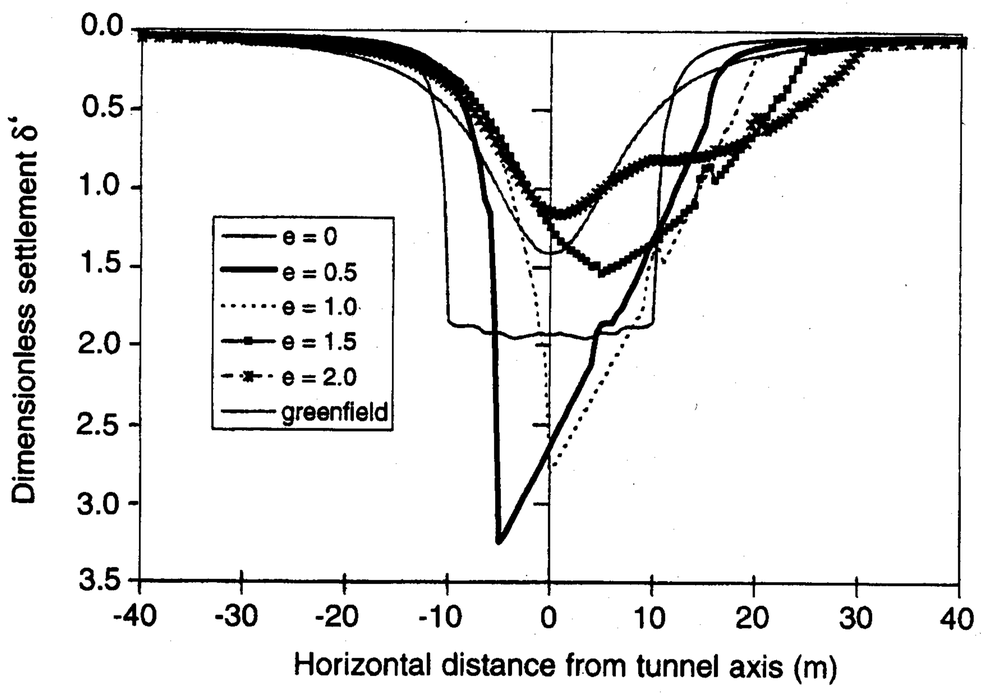

Fig 15. Settlement profiles for varying facade position (light facade, $\gamma_b t$ = 10.0kN/m²)

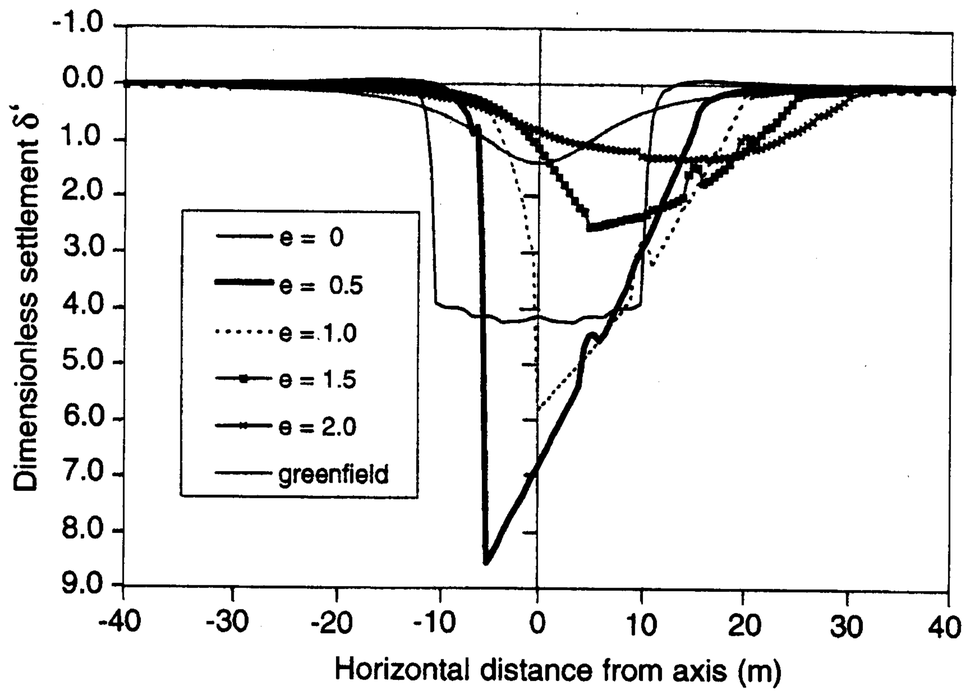

Fig 16. Settlement profiles for varying facade position (heavy facade, $\gamma_b t$ = 20.0kN/m²)

overall trough is still controlled by the excavation. For the heavy facade, its weight has the dominant effect. This can be seen in the settlement plots in Figs 15 and 16 for $e = 2$.

Varying eccentricity e also affects the horizontal movement in the ground beneath the facade. In the symmetric case ($e = 0$), most of the facade lies in the area where the ground tends to impose a compressive horizontal movement. This movement is reduced by the facade considerably, although some local tensile areas exist owing to the arch forces, as discussed previously. When $e = 0.5$–1.0, the left part of the facade is still in the compressive area and able to resist the ground movement, while the right part follows the tensile ground horizontal movement since it does not have tensile stiffness. When e is 1.5– 2, the whole facade moves into the tensile area and translates with the ground horizontally.

Building behaviour

Stress arches, as seen in the symmetric cases, occur with low facade eccentricities, but gradually disappear as e increases.

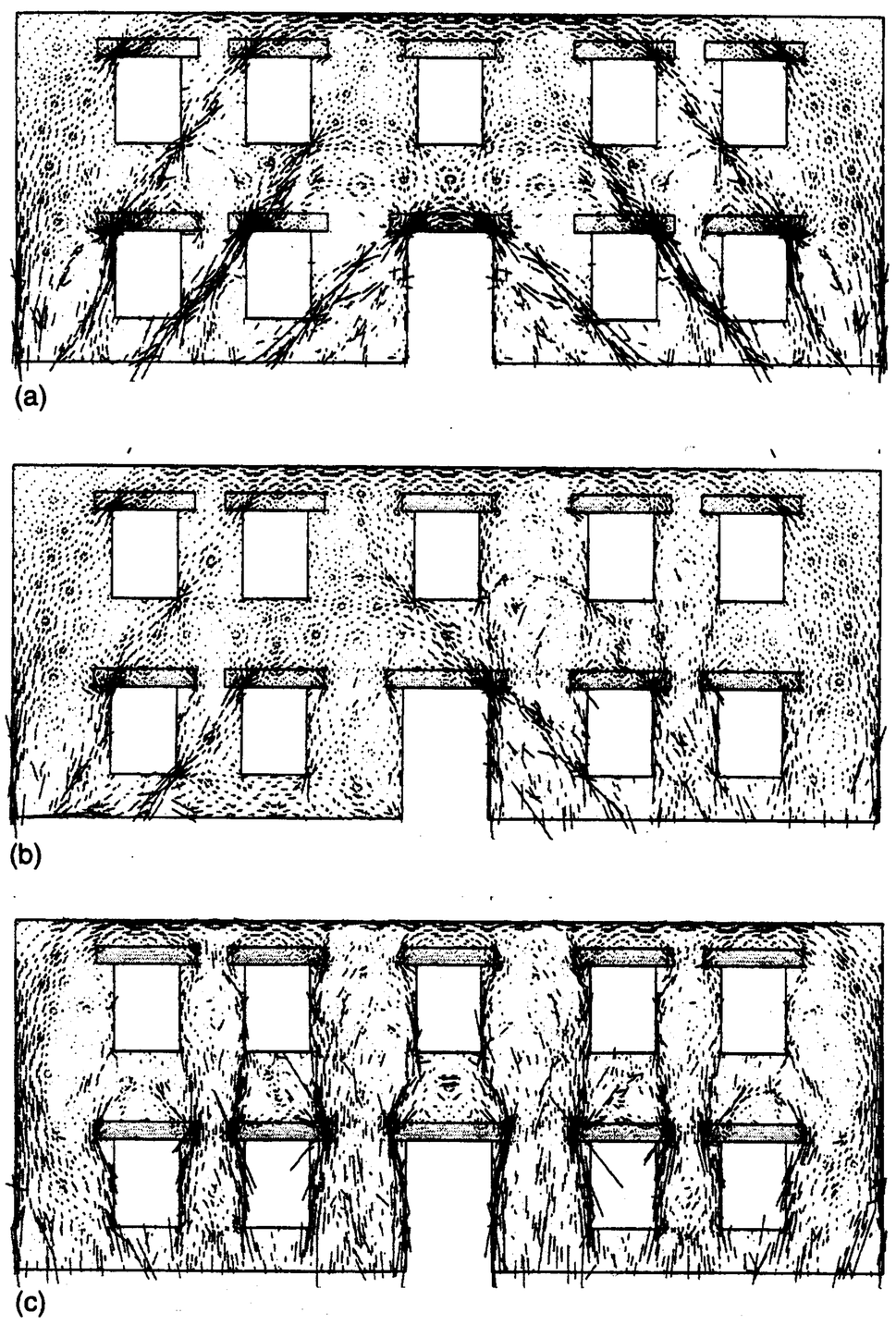

Fig 18. Stress trajectories in light facade for (a) $e = 0$, (b) $e = 0.5$, (c) $e = 2.0$ (analyses u223xx)

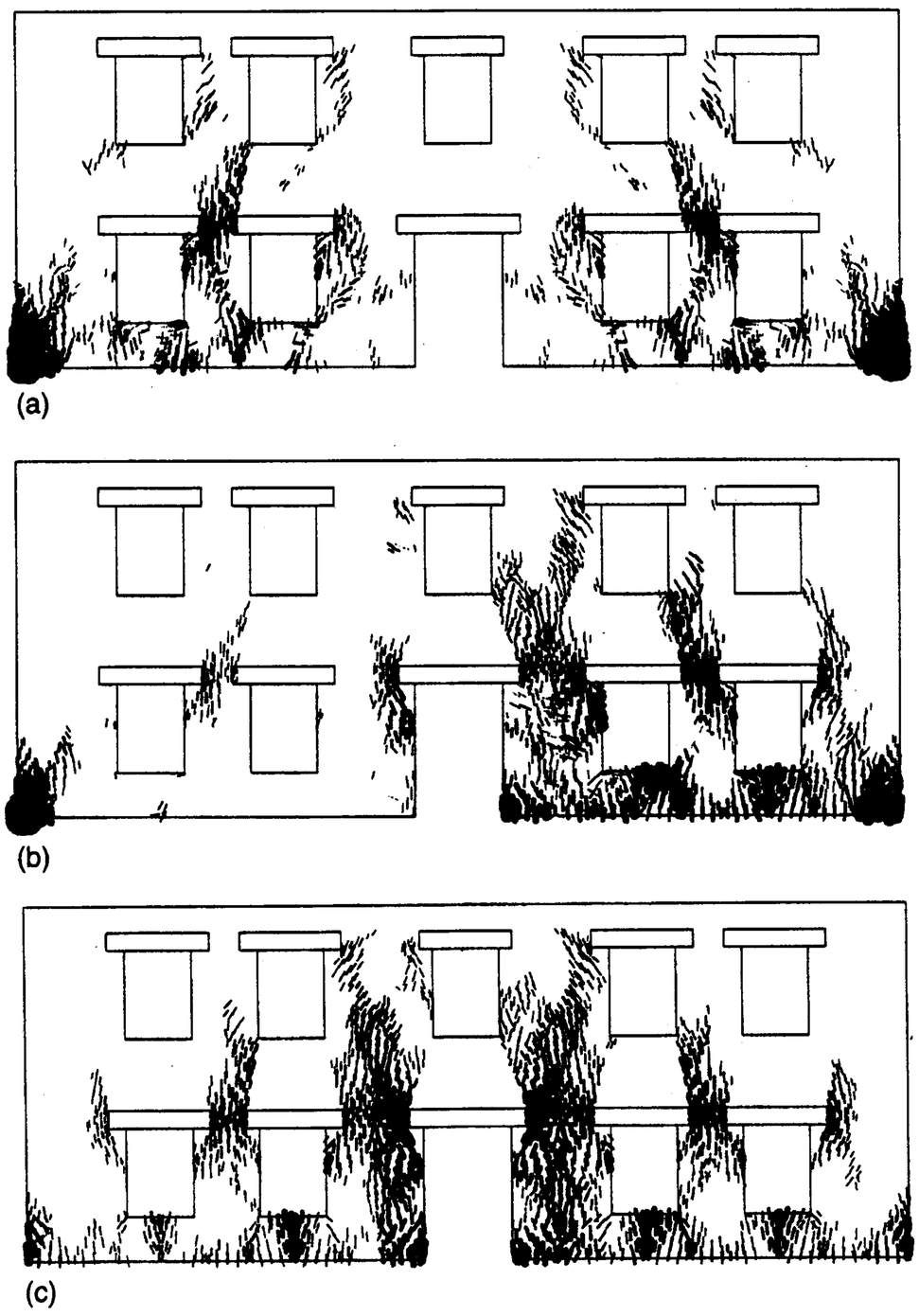

Fig 19. Crack patterns in heavy facade for (a) $e = 0$, (b) $e = 0.5$, (c) $e = 2.0$ (analyses u233xx)

This process is illustrated in Fig 18. Clearly, stress arches cannot be formed when $e = 2$, in the tensile horizontal movement area of the settlement trough, as there is no line of thrust available within the facade to the ground.

Consequently, the cracking patterns change from those along the stress arches to the vertical cracks developed from the bottom of the facade owing to tensile horizontal strains. Cracking patterns exhibiting this change, for $e = 0$, 1, and 2, are shown in Fig 19. When the facade is located remote from the tunnel, it will not experience cracking damage induced by the excavation.

The elastic no-tension facade behaves approximately like a beam with its neutral axis near the top in this local sagging, but horizontally tensile, area. This indicates that, in sagging areas, the building may be modelled as a simple beam but, in hogging areas, stiffness changes, due to cracking, make this idealisation unrealistic.

Conclusions

Analysis of tunnel-induced settlements using a model incorporating a building facade and tunnel excavation, shows that the weight of the building is a key factor in controlling the average settlement underneath. When the facade is located symmetrically over the tunnel, the soil under the building has partially yielded, so that a larger average settlement occurs than in an uncoupled analysis.

Strong arching effects are observed in the masonry facade, which cause redistribution of the weight of the building and change the shape of the settlement trough. For a given weight of building, its stiffness will change the shape of the trough locally beneath it. When stiffness increases, the settlement trough becomes flatter.

In most cases, coupled analyses predict less damage than applying the greenfield trough to the building. However, the large arching force may cause the ground to move outwards horizontally and impose tensile strain at the base of the facade, causing vertical cracks. When the building becomes very heavy, the ground may become unstable and large horizontal movements will occur and the facade will experience more serious damage.

In addition, the position of the masonry facade is another critical factor affecting the ground movements in the combined analysis. When the facade is located partially over the tunnel, it causes larger settlement at the corner near the tunnel than when located symmetrically. It also leads to an appreciable tilt. When the facade is positioned in the overall hogging area (of the settlement profile) the self-weight may change the hogging mode beneath the facade to a local sagging. However, the ground beneath is in horizontal tensile strain, and this prevents the formation of stress arches within the building and instead causes vertical cracks to develop from the base of the facade.

Perhaps the most important conclusion is that the settlement profiles experienced by stiff, heavy buildings bear little resemblance to those predicted for tunnelling under greenfield sites. Although the details of a model of a real structure might be different to the one used in this study (e.g. in terms of foundations), uncoupling the soil and the structural behaviour leads to an unrealistic assessment of damage.

The study presented here is part of a larger one using 2-dimensional models[19],and advanced work, using 3-dimensional modelling, is under way[7]. While this study is limited in scope, it gives an improved understanding of the interaction between a masonry building and the ground during tunnelling. This is largely the result of the complexity of the material models used, for both the ground and the masonry in the facade.

Acknowledgments

This research was funded by EPSRC. The first author was supported by a scholarship from the SBFSS foundation. The authors wish to acknowledge the contribution made to this project by Dr Harvey Burd and Mr Alan Bloodworth.

References

1. Frischmann, W.W., Hellings, J.E., and Snowden, C.: 'Protection of the Mansion House against damage caused by ground movements due to the Docklands Light Railway extension', *Proc. ICE, Geotechnical Engineering*, **107**, No. 2, 1994, p65
2. Mair, R., Taylor, R.N., and Burland, J.B.: 'Prediction of ground movements and assessment of risk of building damage due to bored tunnelling', *Geotechnical Aspects of Underground Construction in Soft Ground*, Rotterdam, Balkema, 1996, p713
3. Boscardin, M., Cording, E.: 'Building response to excavation-induced settlement', ASCE, *Journal of Geotechnical Engineering*, **115**, 1989, p1
4. Potts, D.M., Addenbrooke, T.I.: 'A structure's influence on tunnelling-induced ground movements', Proc. ICE, Geotechnical Engineering, **125**(2), 1996, p109
5. Simpson, B.: 'A model of interaction between tunnelling and a masonry structure', *Numerical Methods in Geotechnical Engineering, Proc. ECONMIG 94*, Rotterdam, Balkema, 1994, p221
6. Addenbrooke, T.I.: 'Holes in one', *Ground Engineering*, **29**, No. 3, 1996, p31
7. Burd, H.J., Houlsby, G.T., Augarde, C.E., and Liu, G.: 'Modelling the effects on masonry buildings of tunnelling-induced settlement', *Proc. ICE, Geotechnical Engineering*, **143**, No. 1, 2000, p17–29
8. Houlsby, G.T.: 'A model for the variable stiffness of undrained clay', *Proc. Int. Symp. on Prefailure Deformation Characteristics of Soils*, Torino, vol.2, Rotterdam, Balkema, 1999, pp443–450
9. Stallebrass, S.E., Taylor, R.N.: 'The development and evaluation of a constitutive model for the prediction of ground movements in overconsolidated clay', Geotechnique, **47**(2), 1997, p235
10. Al-Tabbaa, A., Wood, D.M.: 'An experimentally based bubble model for clay', *Proc. 3rd Int. Conf. Numerical Models in Geomechanics*, 1989, p91
11. St John, H.D., Potts, D.M., Jardine, R.J., and Higgins, K.H.: 'Prediction and performance of ground response due to construction of a deep basement at 60 Victoria Embankment', *Predictive Soil Mechanics, Proc. Wroth Memorial Symp.*, London, Thomas Telford, 1992, p581
12. Ali, S., Page, A.: 'Finite element model for masonry subjected to concentrated loads', ASCE, *J. Struct. Eng.*, **114**(8), 1988, pp1761-1784
13. Pande, G.N., Liang, J., and Middleton, J.: 'Equivalent elastic moduli for brick masonry', *Computers & Geotechnics*, **8**(3), 1989, pp243–265
14. Di Pasquale, S.: 'New trends in the analysis of masonry structures', *Meccanica*, **28**, 1992, pp173–184
15. Gilbert, M., Melbourne, C.: 'Rigid-block analysis of masonry structures', *The Structural Engineer*, **72**, No.21, November 1994, pp356–361
16. Houlsby, G.T. Liu, G., and Augarde, C.E.: 'A tying scheme for imposing displacement constraints in finite element analysis' *Communications in Numerical Methods in Engineering*, **16**(10), October 2000, 721-732
17. Augarde, C.E.: 'Numerical modelling of tunnelling processes for assessment of damage to buildings', *DPhil. thesis*, Oxford University, 1997
18. Davis, E.H., Gunn, M.J., Mair, R.J., and Seneviratne, H.N.: 'The stability of shallow tunnels and ground openings in cohesive material', *Geotechnique*, 30, 1980, pp397–416
19. Liu, G.: 'Numerical modelling of damage to masonry buildings due to tunnelling', *DPhil thesis*, Oxford University, 1997